Patterns of mesozooplankton community composition and vertical fluxes in the global ocean

Yawouvi Dodji Soviadan, Fabio Benedetti, Manoela Brandão, Sakina-Dorothée Ayata, Jean-Olivier Irisson, Jean-Louis Jamet, Rainer Kiko, Fabien Lombard, Kissao Gnandi, Lars Stemmann

Patterns of mesozooplankton community composition and vertical fluxes in the global ocean

Yawouvi Dodji Soviadan[1,6], Fabio Benedetti[2], Manoela C. Brandão[1,3], Sakina-Dorothée Ayata[1,7], Jean-Olivier Irisson[1], Jean Louis Jamet[5], Rainer Kiko[1], Fabien Lombard[1,4], Kissao Gnandi[6], Lars Stemmann[1,*]

1 Sorbonne Université, CNRS, Laboratoire d'Océanographie de Villefranche, 06230 Villefranche-sur-mer, France.
2 Environmental Physics, Institute of Biogeochemistry and Pollutant Dynamics, ETH Zürich, Universitätstrasse 16, 8092 Zürich, Switzerland.
3 Institut Français de Recherche pour l'Exploitation de la Mer, Centre Bretagne, 29280 Plouzané, France.
4 Institut Universitaire de France (IUF), Paris, France
5 Université de Toulon, Mediterranean Institute of Oceanology (MIO), AMU-UTLN UM110, Equipe EMBIO. CS 60584, 83041 TOULON Cedex 9, FRANCE
6 Département de Géologie, Université de Lomé, Togo.
7 Sorbonne Université, CNRS, IRD, MNHN, Laboratoire d'Océanographie et du Climat: Expérimentations et Approches Numériques (LOCEAN-IPSL), Paris, France
.

Corresponding author*

Abstract

Vertical variations in physical and chemical conditions drive changes in marine zooplankton community composition. In turn, zooplankton communities play a critical role in regulating the transfer of organic matter produced in the surface ocean to deeper layers. Yet, the links between zooplankton community composition and the strength of vertical fluxes of particles remain elusive, especially on a global scale. Here, we provide a comprehensive analysis of variations in zooplankton community composition and vertical particle flux in the upper kilometer of the global ocean. Zooplankton samples were collected across five depth layers and vertical particle fluxes were assessed using continuous profiles of the Underwater Vision Profiler (UVP5) at 57 stations covering seven ocean basins. Zooplankton samples were analysed using a Zooscan and individual organisms were classified into 19 groups for the quantitative analyses. Zooplankton abundance, biomass and vertical particle flux decreased from the surface to 1000m depth at all latitudes. The zooplankton abundance decrease rate was stronger at sites characterised by oxygen minima (< 5µmol O_2.kg^{-1}) where most zooplankton groups showed a marked decline in abundance, except the jellyfishes, molluscs, annelids, large protists and a few copepod families. The attenuation rate of vertical particle fluxes was weaker at such oxygen-depleted sites. Canonical redundancy analyses showed that the epipelagic zooplankton community composition depended on the temperature, on the phytoplankton size distribution and the surface large particulate organic matter while oxygen was an additional important factor for structuring zooplankton in the mesopelagic. Our results further suggest that future changes in surface phytoplankton size and taxa composition and mesopelagic oxygen loss might lead to profound shift in zooplankton abundance and community structure in both the euphotic and mesopelagic ocean. These changes may affect the vertical export and hereby the strength of the biological carbon pump

Keywords: Zooplankton, biological carbon pump, Epipelagic, Mesopelagic, Community structure, Particle flux, Attenuation rates, Oxygen Minimum Zone.

Introduction

The upper kilometer of the ocean constitutes a habitat where most of the organic carbon produced by the phytoplankton in the epipelagic layer (0-200m) sinks into the mesopelagic layer (200-1000m) while being progressively consumed and respired. Within the wide size spectrum of planktonic organisms (0.02µm-2m), mesozooplankton (0.2-20mm) are a pivotal component of marine trophic webs impacting the Biological Carbon Pump (BCP) through their feeding, vertical migration, and the production of faecal pellets (Steinberg and Landry, 2017). In a context of global climate change, zooplankton communities experience increasingly stressful conditions through global warming, ocean acidification and deoxygenation (Oschlies et al., 2018; Schmidtko et al., 2017), enhanced water column stratification in the open ocean and modifications in phytoplankton production and community structure (Coma et al., 2009; Kwiatkowski et al., 2019; Richardson, 2008). Long term field surveys have shown how changes in climatic conditions lead to large shifts in surface zooplankton composition (Beaugrand et al., 2019). Future climate warming could further reduce macronutrient supplies in the upper ocean and could therefore lead to a decline in biomass in the tropical open ocean or could cause positive trophic amplification in the polar ocean (Chust et al., 2014). Such changes in biomass may be amplified in the zooplankton through trophodynamic effects, which could greatly alter the fluxes of organic matter into the deeper mesopelagic layers. Modifications of the quantity and quality of the vertical particle flux produced in the surface layers could trigger substantial changes in mesozooplankton abundance and composition. In addition, the expansion of Oxygen Minimum Zones (OMZ) (Schmidtko et al., 2017; Stramma et al., 2010) may further constrain the spatial distribution of the numerous zooplankton taxa that are sensitive to dissolved oxygen levels (Ekau et al., 2010; Kiko et al., 2020; Kiko and Hauss, 2019; Seibel, 2011; Wishner et al., 2020, 2018). Therefore, understanding the variations of zooplankton biomass and diversity in the epi- and mesopelagic is essential to better understand the impact of global climate change on the properties of marine ecosystems.

However, mesopelagic zooplankton communities remain critically under-sampled compared to the epipelagic ones, as most collections are in the first 200m of the water column (Everett et al., 2017). The mesopelagic is still considered a “dark hole” (Robinson et al., 2010; St John et al., 2016) as the gaps in sampling lead to critical holes in knowledge regarding the functioning of mesopelagic ecosystems and how they are controlled by the organic matter fluxing from the euphotic zone. Local to regional field studies reported that the abundance of mesozooplankton decreases exponentially with depth, in parallel with

substantial changes in species diversity and genus composition that remain poorly resolved (Bode et al., 2018; Brugnano et al., 2012; Hernández-León et al., 2020; Koppelmann et al., 2005; Kosobokova and Hopcroft, 2010; Yamaguchi et al., 2004). Some studies reported increases in diversity with depth, with maxima in the meso- to bathypelagic layers (Bode et al., 2018; Gaard et al., 2008; Kosobokova and Hopcroft, 2010; Yamaguchi et al., 2004), whereas other studies reported either the opposite diversity pattern or even an absence of vertical patterns due to large spatio-temporal variability (Gaard et al., 2008; Hidalgo et al., 2012; Palomares-García et al., 2013; Wishner et al., 2008). Such mismatch between observations might be related to the wide range of environmental conditions sampled using a variety of sampling gears that make inter-comparisons difficult. One recent global analysis of zooplankton vertical distribution in inter-tropical regions showed that in this narrow latitudinal band the vertical dimension was the main structuring pattern suggesting that midwater processes mediated by zooplankton may not change between oceans at those latitudes (Fernández de Puelles et al., 2019). How these changes relate to the vertical flux and also across the full latitudinal band is poorly understood because plankton observations and biogeochemical studies have usually been carried out by distinct scientific communities. Recent interdisciplinary cruises have taken place, providing more integrated knowledge on the importance of zooplankton to carbon sequestration (Guidi et al., 2016; Kiko et al., 2020; Steinberg and Landry, 2017; Stukel et al., 2019). No global study has yet been able to analyse community-level variations in zooplankton abundances, biomass and community composition in conjunction with assessments of vertical particle flux in the upper kilometre of the global ocean.

Here, a homogeneous dataset of community-level zooplankton images generated from the TARA Oceans expeditions is explored together with associated measurements of their contextual environmental conditions to: (i) test whether zooplankton communities present consistent vertical variations in abundance and composition across the oceans and in different latitudinal bands, and (ii) investigate the main drivers of such vertical gradients and how they are coupled to the surface phytoplankton and estimates of particle flux. The TARA Oceans expedition collected over 35000 samples encompassing the whole plankton community (i.e., from viruses to jellyfish) across the global ocean from 2009 to 2013 (Karsenti et al., 2011). Previous studies that analysed the TARA Oceans imaging dataset explored the global latitudinal gradients in richness and composition for the whole plankton community focusing on surface waters (Ibarbalz et al., 2019; Brandao et al., in press). Here, we aim to describe the community composition of mesozooplankton down to 1000m depth on a global scale. As the

imaging techniques used here cannot achieve a species-level identification of the zooplankton community composition, our approach is rather oriented towards larger taxonomic and /or functional groups that may be associated with broad ecological and biogeochemical functions.

Materials and methods

Sampling sites and environmental variables

TARA Oceans took place between 2009 and 2013. Among the 210 stations that were sampled, 57 stations covering 7 ocean basins (Fig. 1) were sampled with a Multinet (Pesant et al., 2015; Roullier et al., 2014), a sampling device with five nets that allows for depth-stratified sampling (see below).

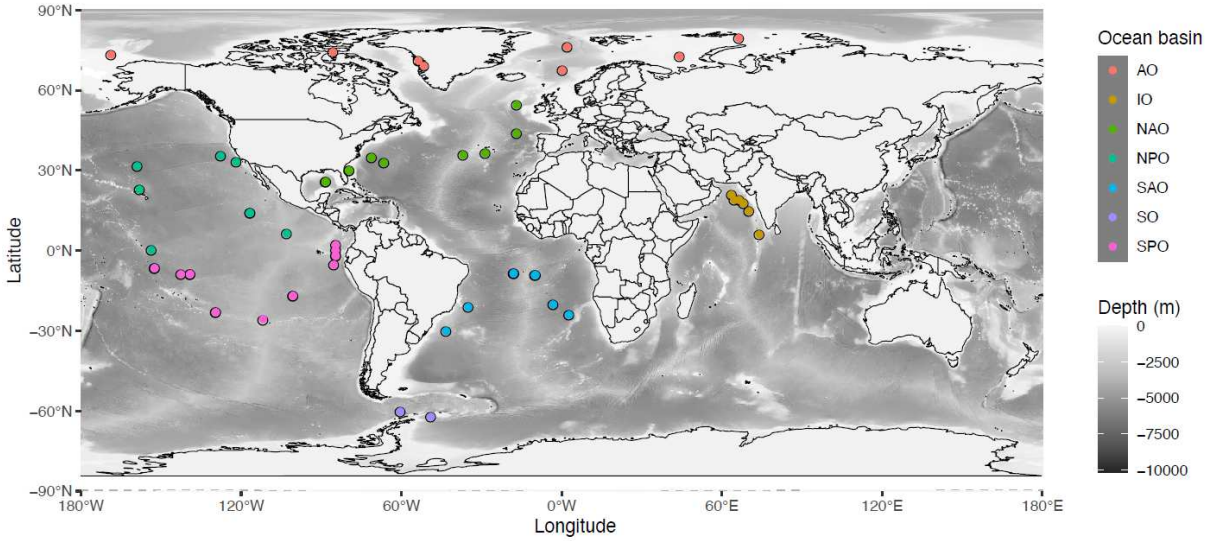

Fig. 1: Location of the 57 stations sampled with the Multinet, grouped by ocean basin: AO=Arctic Ocean, IO=Indian Ocean, NAO=North Atlantic Ocean, NPO=North Pacific Ocean, SAO=South Atlantic Ocean, SO=Southern Ocean or Austral Ocean, SPO=South Pacific Ocean.

A CTD rosette equipped with optical sensors was deployed to measure the physico-chemical parameters within the water column. Temperature and conductivity were measured from the surface to a maximum of 1300 m depth using a Seabird 911 CTD mounted on a Sea-Bird Carousel sampler with 10 Niskin bottles. The following additional sensors were mounted to measure optical properties related to relevant biogeochemical variables: fluorometer (Wetlab ECO-AFL/FL model), dissolved oxygen sensor (model SBE 43), nitrate sensor (ISUS with a maximum rating depth of 1000m Satlantic SA), a 25 cm transmissometer for particles 0.5–20 µm (WETLabs), a one-wavelength backscatter meter for particles 0.5–10 µm

(WETLabs), and an Underwater Vision Profiler 5 (UVP5) for particles >150 µm and zooplankton >600 µm (Hydroptic). Assuming that particle sinking speed increases with size, those particles detected through the backscattering will be referred to as suspended particulate matter (SPM, particles < 10µm in Equivalent Spherical Diameter), while the ones detected by the UVP5 (>150µm in Equivalent Spherical Diameter) will be referred as particles. Vertical particle mass flux (in mg Dry Weight m^{-2} d^{-1}) was calculated from the particle size spectra detected by the UVP5 as in (Guidi et al., 2008). Based on the High Pressure Liquid Chromatography (HPLC) analysis of water collected with Niskin bottles, we used the method of (Uitz et al., 2006) to estimate the contribution (%) of three pigment size classes (microphytoplankton, nanophytoplankton, and picophytoplankton; f_micro, f_nano, and f_pico, respectively) to total phytoplankton biomass in the epipelagic layer. According to the authors, such grouping allows for the description of the broad community composition with f_micro dominated by diatoms, f_nano by chromophytes, cryptophytes and nanoflagellates and f_pico by cyanobacteria, green flagellates and prochlorophytes. The median value of all hydrological and optical data together with imaging data were calculated for each of the five horizontal layers sampled by the Multinet for future data processing. The samples were classified as anoxic, hypoxic and normoxic according to the oxygen minimum value measured within the towed layer. We used a threshold of 5 $\mu mol\ kg^{-1}$ to classify the stations as anoxic (Roullier et al., 2014) and 58.5 $\mu mol\ kg^{-1}$(Bode et al., 2018) to classify them as hypoxic.

Zooplankton sampling, digitization, biomass estimates

A Hydrobios Multinet (with a 300µm mesh and an aperture of 0.25m^2) was used to sample zooplankton (Roullier et al., 2014; Pesant et al., 2015) in five distinct water layers ranging from the surface to occasionally 1300 m depth. The five depth layers were locally defined as a function of the vertical structure of the water column according to the profiles of temperature, salinity, fluorescence, nutrients, oxygen, and particulate matter (Pesant et al., 2015). The Multinet was equipped with a flowmeter to measure the volume of seawater filtered by each net tow (Pesant et al., 2015). Day and night net tows were conducted at ten stations. Sampling at the other stations occurred at day or night, depending on cruise schedule and operational constraints. Once collected, the samples were preserved in a solution of buffered formaldehyde-Borax solution (4%). In the laboratory, the samples were rinsed and split with a Motoda box (MOTODA, 1959). The final split was analysed with the Zooscan imaging system (Gorsky et al., 2010) which allowed a rapid and semi-automatic analysis of zooplankton samples. Few tens of morphological attributes (max and min length, area, grey

leves, ...) are measured on each object and used for the initial prediction. In total, nearly 400,000 images of living zooplankton and detritus and their associated morphological data were obtained by the Zooscan. These images were imported into Ecotaxa, an online platform which allows an automatic prediction of the taxonomic classification of each single image followed by a manual validation/correction. The organisms were then identified manually down to the order, sometimes to the family and rarely down to the genus level. All copepods were sorted at the family level apart from the smallest copepods that cannot be recognised at the family level from the image. They were all grouped into one category called Other-copepoda or other-Calanoida if their morphological features permitted classifying them as Calanoida. This initial sorting allowed classifying zooplankton into 119 taxa. As many taxa showed a very small contribution to total zooplankton abundance, the 119 taxa were grouped into 19 taxonomic groups (Table 1). Those include all the major zooplankton groups that are frequently observed in the oceans. To investigate vertical patterns in mesozooplankton abundance, these 19 groups were further aggregated into eight groups representing a combination of taxonomic and functional classification (Table 1).

Once the zooplankton images were sorted, Ecotaxa enabled us to extract the concentration and the biovolume of each mesozooplankton group at every station and for every net tow, while accounting for the Motoda fraction and the volume sampled. The biovolume was computed for each individual zooplankton using the minor and major length axes assuming a prolate ellipsoidal shape (Gorsky et al., 2010). The biomass was calculated for the 8 large groups using the equations for the different taxa :

$$Body\ Weight(\mu C) = aS^b \quad (1)$$

where S is body area in mm^2. Taxon-specific area-to-dry mass conversion factors (Lehette and Hernandez-Leon, 2009) and dry mass to carbon (C) conversion factors (Kiørboe, 2013) were used to calculate the biomass and C content of each zooplankton organism scanned. Taxonomic units and biomass conversion factors used are listed in Table 2. For large protists the conversion factor was adjusted to $0.08\ mgC\ mm^{-3}$ (Biard et al., 2016).

Shannon diversity index (H') was calculated based on the relative abundances of the 119 taxa for each sample as follows:

$$H' = -\sum_i^n \quad p_i log p_i \quad (2)$$

where p_i is relative abundance of each taxa in one sample and log is the natural logarithm.

Analyzing the vertical distribution of zooplankton and particles

Vertical attenuation rates of zooplankton (abundance and biomass) and estimated particle fluxes were estimated, from the five sampled layers for zooplankton and from the 5 meter resolution profile of estimated vertical flux using the following equation :

$$X = X_0(Z/Z_0)^b \quad (3)$$

where X represents the zooplankton abundance, the zooplankton biomass or the particle vertical flux at the depth level Z, $X_0$the zooplankton biomass or abundance and vertical particle flux at the depth Z_0 (chosen as median depth of the surface net) and b the slope taken as a proxy of the attenuation rate of zooplankton biomass zooplankton abundance or particle flux. In the rest of the manuscript, A_zoo represents the slope b of vertical profile for zooplankton abundance, B_zoo the slope b of vertical profile for zooplankton biomass, A_flux the slope b of vertical profile for particle flux, and P_flux1, P_flux2 and P_flux3 the particle flux in respectively the epipelagic, upper and lower mesopelagic. To analyse latitudinal patterns in attenuation rates, the slope values were separated into three latitudinal bands based on the latitudinal position of their corresponding sampling stations: intertropical (0°-30°), temperate (30-60°) and polar (60°-90°). The intertropical stations gathered both OMZ and non-OMZ stations, which allowed us to analyse the effect of oxygen depletion on zooplankton and particles. Non-parametric variance analyses (Kruskal and Wallis tests) were performed to test for differences in slope values (i.e. zooplankton and particles attenuation rates) between latitudinal bands.

Multivariate analysis of community composition

To explore the response of zooplankton community composition to environmental drivers across depth layers, the non-interpolated abundances of the 19 taxonomic groups mentioned above were aggregated into three layers: the epipelagic layer (0-200m), the upper mesopelagic layer (200-500m) and the lower mesopelagic layer (500-1000m). To analyse separately the three depth layers, the samples collected in overlapping layers (18.59% of the total samples) were not included in the statistical analysis (Table S1). To characterise the environmental conditions of each layer at each sampling station the median values of the following contextual environmental variables were used: temperature (T), salinity (S), oxygen (O_2), nitrate concentration (NO_3), chlorophyll *a* concentration (Chl_*a*), phytoplankton size fractions ($f_{\_micro}$, $f_{\_nano}$, and $f_{\_pico}$), concentration of suspended particles (SPM) and particle flux (P_Flux). The measurements of all these environmental variables are available on PANGAEA (https://doi.org/10.1594/PANGAEA.840721).

To estimate the strength of the Diel Vertical Migration (DVM) at 10 stations, pairwise Wilcoxon tests were performed to compare in each layers the abundance and biomass of each taxa between day and night. For those 10 same pairs of stations, we used an analysis of similarities (ANOSIM) to test for significant variations in community composition between day and night samples. The ANOSIM tested whether the inter-groups difference (day and night groups) was higher than the intra-groups difference, by providing an R coefficient. An R coefficient close to one suggests dissimilarity between groups, while R value close to zero suggests an even distribution of high and low ranks within and between groups. An R value below zero suggests that dissimilarities are greater within groups than between groups (Clarke and Gorley, 2001). ANOSIM tests were performed within each layer using log-transformed (where log is the natural logarithm) abundances and Bray-Curtis distance among stations.

For each depth layer, a canonical redundancy analysis (RDA) was performed based on the abundances of the 19 mesozooplankton groups and the above-mentioned environmental variables to explore the explanatory power of these variables in structuring the mesozooplankton community. The RDA is an extension of the multiple regression analysis applied to multivariate data (Legendre and Legendre, 1998). It allows representing the response variables (abundances of the 19 mesozooplankton groups) in a "constrained" reduced space, i.e., constructed from the explanatory variables (the environmental variables). For each RDA, the following variables were used as "supplementary variables" of the analysis in order to visualize their correlation with the environmental structuring of the mesozooplankton community (i.e., to visualise their position in the RDA space): attenuation of particle flux (A_flux), attenuation of zooplankton abundance (A_zoo), attenuation of zooplankton biomass (B_zoo) and the Shannon index (*H'*). Beforehand, a Hellinger transformation was performed on the mesozooplankton abundances. A preliminary RDA based on all samples together showed a very strong effect of depth on mesozooplankton community composition (Fig. S1). Therefore, to avoid such a strong effect of depth on the community composition analysis, three separate RDAs were performed on each of the three layers defined above. Significant axes were identified using the Kaiser-Guttman criterion (Legendre and Legendre, 1998).

Data manipulation and statistical analyses were performed with Matlab 2018b (MATLAB 9.5) for the vertical profiles of abundance and biomass and statistical test (Wilcoxon test, Kruskal-wallis test), R environment v3.5.1 (using the following packages: vegan version 2.5-5, ggplot2 version 3.1.1, ggrepel version 0.8.0 and ggfortify version 0.4.7)

for the redundancy analysis and PRIMER6 (Version 6.1.12) and PERMANOVA+ (Version 1.0.2) for the ANOSIM test.

Results

Day night variability

In each layer, the comparison between day/night of the taxonomic groups indicated that only a few groups (Euphausiidae, Metridinidae, Corycaeidae and Cnidaria for abundance; Eumalacostraca and Ostracoda for biomass) showed significant differences in either the surface layer or the upper mesopelagic layer (Table S1). Nonetheless, the ANOSIM found no significant differences in the community composition between the day and night samples at the community-level (R0-200m = -0.039; R200-500m = -0.008; R500-1100m = -0.006). The same analyses based on biomass also indicated no significant differences (R0-200m = 0.018; R200-500m = -0.051; R500-1100m = 0.087). As a consequence, all further analyses were carried out without making any distinctions between day and night samples.

Vertical patterns in zooplankton total abundance and biomass and particle flux

On a global scale, zooplankton abundance and biomass decreased exponentially with depth (Fig. 2) in the different latitudinal bins. Abundance and biomass decrease rate with depth and were correlated (r^2=0.342, p=4.6*10^{-5}) but the biomass attenuation rate estimates were systematically lower than the attenuation based on the abundance profiles. On average, polar waters showed increased zooplankton abundance and biomass compared to the stations located in the tropics. In the epipelagic layer, abundances and biomass ranged from 1 to 5000 ind m^{-3} and 0.05 to 200 mg C m^{-3} while in the mesopelagic they were reduced to 0.05 to 450 ind m^{-3} and 0.005 to 40 mg C m^{-3}. Copepods were the most abundant being 85% and 65% of the abundance and biomass in the epipelagic, 85 and 76% in the upper mesopelagic and 95% and 97% in the lower pelagic (Table 3). The estimated vertical flux also decreased with depth in all latitudinal bands. On average, polar waters showed higher fluxes compared to the stations located in the tropics.

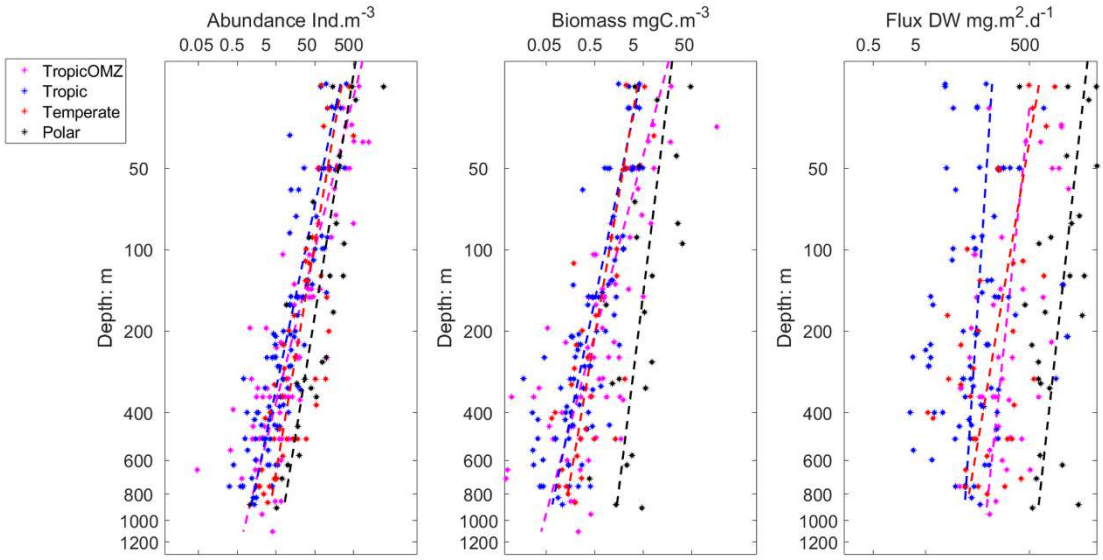

Fig. 2: Vertical distribution of zooplankton biomass, abundance and particle flux in different latitudinal bands. Dotted lines represent the fitted regression for each latitudinal band (equation 3). The parameters are given in table 4.

The attenuation rates of zooplankton abundance and biomass with depth were stronger than the attenuation rates of the vertical particle flux (Fig. 3A, B and C, Table 4). The decrease rates in zooplankton vertical abundance and biomass are more pronounced in OMZ stations compared to the non-OMZ stations. Yet, such difference was found to be significant only when the vertical decrease rates were calculated from abundances. In general, zooplankton attenuation rates decreased with latitude whereas the attenuation rates of particle fluxes increased with latitude (Fig. 3, Table 3). A non-parametric variance analysis (Kruskal-Wallis test) of the attenuation rate revealed significant differences in the attenuation rates of zooplankton abundances between the anoxic tropical stations and the temperate and polar ones, but not with the other tropical stations (Table 4). No statistical difference between regions was found. The attenuation rate of vertical flux was weaker at the OMZ sites compared to the non OMZ ones but this difference was not significant (Fig. 3B).

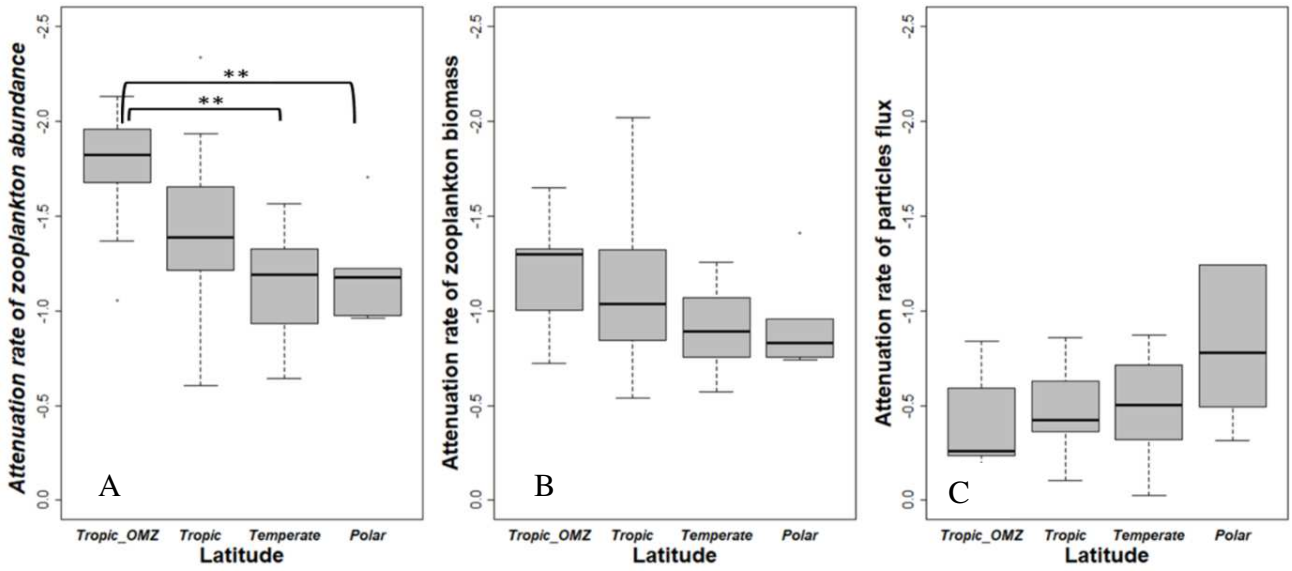

Fig. 3: Distributions of attenuation rates per latitudinal band (Tropical, Tropical OMZ, Temperate, and Polar). A: Attenuation rate of zooplankton abundance (A_zoo). B: Attenuation rate of zooplankton biomass (B_zoo). C: Attenuation rate of particle flux (A_flux). (**) means significant Kruskal-Wallis test with $p < 0.01$ (Table 5).

Structuring of the epipelagic community composition.

In the epipelagic layer (0 – 200 m depth), the environmental variables explained 32.71% of the total variance in mesozooplankton groups' abundances. The first RDA axis (RDA1, 57.18 % of constrained variance) opposed the samples from polar waters, and especially those from the Arctic dominated by Calanidae and crustacean larvae (RDA1 > 0), to the tropical samples presenting more even contributions from most of the remaining groups: Protista, Eumalacostraca, Annelida, Amphipoda, Corycaeidae, Chaetognatha, Euphausiacea, Oithonidae, Ostracoda, Oncaeidae, Calanoida (RDA1 < 0). RDA1 was negatively scored by temperature and salinity and positively scored by vertical particle flux, microphytoplankton contribution, suspended particle concentration, dissolved oxygen concentration and chlorophyll *a* concentration. Among the supplementary variables, the attenuations of the particle flux and of the zooplankton biomass were positively correlated with RDA1, while the attenuation of the zooplankton abundance and the Shannon index were negatively correlated to RDA1. RDA2 (13.1% of constrained variance) opposed the samples from the Indian Ocean and North Atlantic Ocean that present higher abundances of Cnidaria, Mollusca, Tunicata and Cladocera (RDA2 < 0) to those samples from the Southern Ocean presenting higher abundances of Annelida, Euphausiacae, Amphipoda and Other Copepoda

(RDA2 > 0). RDA2 was positively scored by nitrate concentrations and the relative contribution of nanophytoplankton. It was negatively scored by the concentration of suspended particles and the relative contribution of microphytoplankton. All supplementary variables were negatively correlated with RDA2.

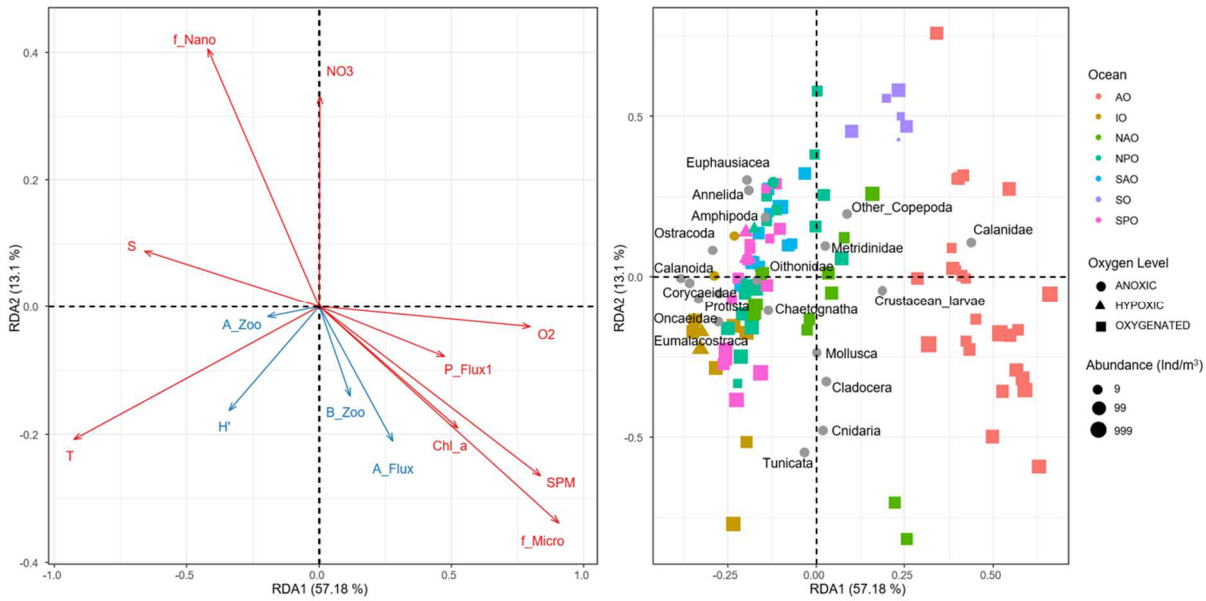

Fig. 4: RDA on the epipelagic communities with the factors in the left panel and samples and taxa in the right panel. Each colored dot corresponds to a sample, i.e., one net at one depth at one station while the taxa are given as grey dots. The red arrows correspond to the quantitative environmental variables in RDA space: f_pico, f_nano and f_micro correspond to the relative contribution (%) of pico-, nano- and micro-phytoplankton to total phytoplankton biomass, O2 = dissolved oxygen concentration (µmol/kg), Chl_a = Chlorophyll a concentration (mg/m3), SPM = suspended particles matter (m/sr), T = temperature (°C), Sal = salinity, NO3 = nitrate concentration (mol/kg), Z = depth (m)) and P_Flux= particulate flux ($mg.m^{-2}.d^{-1}$). Grey dots mark the projection of the zooplankton groups abundance ($ind.m^{-3}$). Supplementary variables estimated for the epipelagic layer are represented with blue arrows: attenuation of particle flux (A_flux), attenuation of zooplankton abundance (A_zoo), attenuation of zooplankton biomass (B_zoo) and the Shannon index (H'). Colors correspond to the ocean basin where the samples were taken: AO = Arctic Ocean, IO = Indian Ocean, NAO = North Atlantic Ocean, NPO = North Pacific Ocean, SAO = South Atlantic Ocean, SO = Southern Ocean, SPO = South Pacific Ocean. Shapes illustrate oxygen level, Anoxic: [O_2] <5µmol/kg; Hypoxic: 5µmol/kg< [O_2] <58.5µmol/kg and oxygenated: [O_2]>58.5µmol/k).

Structuring of the upper mesopelagic community composition.

In the upper mesopelagic layer (200 to 500 m depth), the environmental variables explained 29% of the total variance in mesozooplankton groups' abundances. Again, the first

RDA axis (RDA1, 36.33% of constrained variance) mainly opposed the polar samples dominated by Calanidae copepods, and characterized by higher concentrations of suspended particle, particle flux (both from surface and upper mesopelagic layer), and higher dissolved oxygen concentrations (RDA1 > 0), from the samples characterized by more diverse zooplankton communities (mainly Corycaeidae, small Calanoida, Oncaeidae) and correlated to higher temperature, higher salinity and a higher relative contribution of the nanophytoplankton (RDA1 < 0). Similarly, to what was observed for the epipelagic layer, among the supplementary variables, the attenuations of the particle flux and of zooplankton biomass were positively correlated with RDA1, while the attenuation of zooplankton abundance and the Shannon index were negatively correlated to RDA1. RDA2 (24.72% of constrained variance) opposed the anoxic samples from the Indian Ocean presenting higher abundances of Tunicata, Annelida, Protista, Mollusca, Oithonidae and Cnidaria (RDA2 < 0) to the oxygenated ones displaying higher abundances of Ostracoda, Eumalacostraca, crustacean larvae, other Copepoda, Chaetognatha and Euphausiacea (RDA2 > 0). Samples from the Arctic Ocean were dominated by large copepods from the Calanidae and Metridinidae families. Samples from the Pacific and Atlantic Oceans were dominated by other Copepoda, Eumalacostraca, Ostracoda, Euphausiacea, Chaetognatha and crustacean larvae. Higher attenuation rates of zooplankton biomass and particle flux were found in polar samples whereas higher zooplankton attenuation rates were found in warmer waters, especially at OMZ stations. Again, samples from the tropical upper mesopelagic layers displayed more diverse communities the extra-tropical regions. The distribution of the supplementary variables along RDA2 differed from what was observed for the epipelagic layer, as the supplementary variables, except the attenuation of the zooplankton abundances, were positively correlated to RDA2.

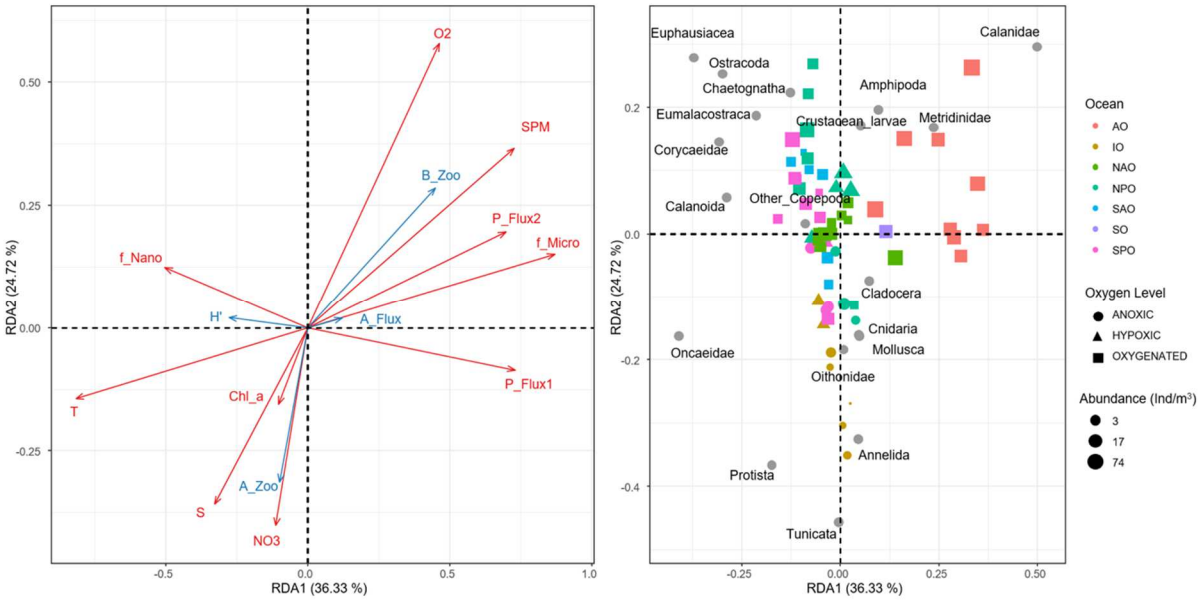

Fig. 5: RDA performed on the upper mesopelagic abundances with the factors in the left panel and samples and taxa in the right panel. Each colored dot corresponds to a sample, i.e., one net at one depth at one station while the taxa are given as grey dots. The orange arrows correspond to the quantitative environmental variables (see legend of Fig. 4). Anoxic: [O_2] <5µmol/kg; Hypoxic: 5µmol/kg< [O_2] <58.5µmol/kg and oxygenated: [O_2]>58.5µmol/kg). Supplementary variables estimated for the upper mesopelagic layer are represented with blue arrows: attenuation of particle flux (A_flux), attenuation of zooplankton abundance (A_zoo), attenuation of zooplankton biomass (B_zoo) and the Shannon index (*H'*).

Structuring of the lower mesopelagic community composition

In the lower mesopelagic layers (500 to 1000 m depth), the environmental variables explained 29.46 % of the total variance in mesozooplankton groups' abundances. The first RDA axis (RDA1, 35.14 % of constrained variance) opposed the stations from the Arctic and North Atlantic Oceans characterized by higher dissolved oxygen concentrations, higher suspended particle concentrations (RDA1 > 0), from the anoxic and nitrate-rich stations from the Indian Ocean (RDA1 < 0). The former stations were characterized by higher abundances of Calanidae, Calanoida, Metridinidae, crustacean larvae, Ostracoda and Amphipoda, whereas the latter were characterized by higher abundances of Tunicata, Annelida, Eumalacostraca and other Copepoda. RDA2 (22.08 % of constrained variance) separated the colder and less salty stations of the Southern Atlantic Ocean (RDA2 < 0) from the warmer, saltier stations (RDA2 > 0) of the North Atlantic and the Indian Oceans that are characterized by less diverse zooplankton communities. The stations that sampled the oxygenated waters of the North Atlantic and Arctic Oceans were dominated by large copepods of the Metridinidae and Calanidae families, as well as most of the small other Calanoida (i.e. those smaller copepods

that could not recognized at a more detailed taxonomic level) in addition to Ostracoda, Amphipoda, and crustacean larvae. Oxygenated stations from the South Atlantic Ocean (SAO) were characterized by higher abundances of Chaetognatha, Corycaeidae, Euphausiacea, Cnidaria, Mollusca, Oithonidae, Oncaeidae and Protista. Samples taken in the OMZ of the Indian and North Pacific Oceans displayed higher abundances of other Copepoda, Tunicata, Annelida, Eumalacostraca and Protista. Higher mesozooplankton biomass and stronger particle flux attenuation rates were found in the normoxic waters while higher zooplankton attenuation rates were observed at the stations that sampled an OMZ. The distribution of the supplementary variables showed similar association with environmental variables as in the upper mesopelagic.

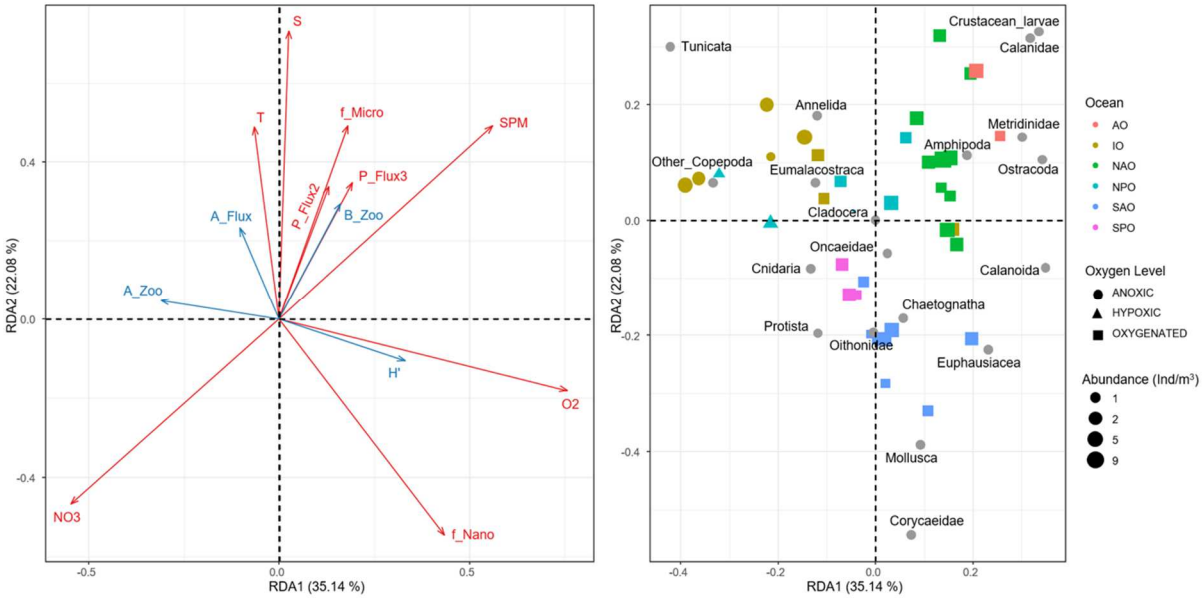

Fig. 6: RDA performed on the lower mesopelagic abundances with the factors in the left panel and samples and taxa in the right panel. Each colored dot corresponds to a sample, i.e., one net at one depth at one station while the taxa are given as grey dots. The orange arrows correspond to the quantitative environmental variables (see legend of Fig. 4). Anoxic: $[O_2]$ <5µmol/kg; Hypoxic: 5µmol/kg< $[O_2]$ <58.5µmol/kg and oxygenated: $[O_2]$>58.5µmol/kg). Supplementary variables estimated for the lower mesopelagic layer are represented with blue arrows: attenuation of particle flux (A_flux), attenuation of zooplankton abundance (A_zoo), attenuation of zooplankton biomass (B_zoo) and the Shannon index (*H'*).

Discussion

The present global analysis of spatial patterns of the mesozooplankton community and their relationship with the strength of the vertical particle flux is based on zooplankton abundance and biomass and vertical particles flux estimated using state-of-the-art imaging techniques (Zooscan and UVP5). The rigorous quality control (see Supplementary Material) allows to depict correlations between zooplankton and particle flux, two important components of the biological carbon pump (BCP). Notably the study allows to infer global ecological patterns in the epipelagic and mesopelagic layers, the coupling between these two layers in oxygenated, hypoxic and anoxic situations. Diel Vertical Migration in zooplankton at global scale and it's relationships with particle vertical flux could not be investigated because the net sampling was not designed to address the DVM globally. However, at 10 occasions, day and night sampling was performed and revealed diel variability for few taxa but no change in the community composition (see Supplementary Material). As a consequence, all further analyses were carried out without making any distinctions between day and night samples.

Important environmental factors for the mesozooplankton community composition in the epipelagic layer

High latitude marine ecosystems are characterised by a combination of lower species diversity and shorter food webs (Laws, 1985; Stempniewicz et al., 2007) sustained by higher concentrations of large microphytoplankton cells (diatoms). On the contrary, low latitude ecosystems are featured by more complex and diverse food webs (Saporiti et al., 2015; Uitz et al., 2006, p. 200) adapted to lower production rates ensured by smaller cells (i.e. pico- and nanoplankton). How the dynamics of zooplankton community composition and vertical particle flux follow this scheme remains more elusive. Previous field-based studies reported peaks in zooplankton species richness in the tropics (Rombouts et al., 2010; Rutherford et al., 1999; Yasuhara et al., 2012), which is in line with the above-mentioned theory that the tropical food-depleted regions promote more complex food-webs with higher species richness. Our RDAs results supports the view that, on a global scale, temperature and the production regime of surface ecosystems are the main drivers of zooplankton community structure in the epipelagic layer. Therefore, in the epipelagic layers, less abundant and more diverse zooplankton thrive in warm, pico- and nanophytoplankton-dominated waters contrary to the polar waters where zooplankton is much more abundant but less diverse. Polar waters are characterised by a higher contribution of microphytoplankton to total phytoplankton

biomass and higher concentrations of particles. Our results also indicate that the two polar communities are not completely alike, as the Arctic is dominated by calanoid copepods while euphausiids and small undetermined copepods dominate in the few stations sampled in the Southern Ocean. Such differentiation has been previously shown by several authors who found that Arctic zooplankton were dominated by *Calanus* spp. (Balazy et al., 2018; Hirche and Mumm, 1992), whereas it was shown that Antarctic zooplankton were dominated by euphausiids, small calanoids, cyclopoids (i.e. *Oithona* spp., *Oncaea* spp.) and salps (Park and Wormuth, 1993; Pinkerton et al., 2020; Quetin et al., 1996; Ross et al., 2008; Steinberg et al., 2015).

Important environmental factors for the mesozooplankton community structure in the mesopelagic layer

The RDA displayed similar general patterns in both the upper and lower mesopelagic layers with the stations in the Indian Ocean (with low zooplankton concentration in low oxygen) and Arctic Ocean (with high zooplankton concentration in oxygenated conditions) being in all layers well separated from the other stations in the remaining ocean. The highest mesopelagic zooplankton concentrations were found at stations associated with high microphytoplankton concentrations in the epipelagic and high particle flux, suggesting a strong impact of surface production regime on the mesozooplankton in the mesopelagic (Hernández-León et al., 2020). The inter-basin differences in zooplankton concentration and community composition was slightly lower in the lower mesopelagic compared to the upper mesopelagic, probably due to the more homogeneous habitat (Fernández de Puelles et al., 2019).

In general, stations associated with anoxic or hypoxic conditions at midwater depth displayed lower zooplankton concentrations in the mesopelagic and different community composition from oxygenated layers. The stations that sampled the tropical OMZ showed higher proportions of gelatinous carnivorous zooplankton (Cnidaria), gelatinous filter feeders (Tunicata), Mollusca and small omnivorous grazers (Cladocera). Anoxic or strongly hypoxic conditions in the mesopelagic may have selected for those taxa adapted to low oxygen (Vaquer-Sunyer and Duarte, 2008). In mesopelagic oxygenated waters, the stations of the Tropical Pacific Ocean displayed a higher diversity stemming from the higher and relatively even abundances of large protists (i.e. Rhizaria and Foraminifera), chaetognaths, crustaceans (Ostracods, Euphausiacea, Eumalacostraca, Amphipoda), and various copepod families (Corycaeidae, Oithonidae, Oncaeidae, small Calanoida). These zooplankton communities

were associated with oligotrophic conditions at surface (Fig. 4), lower zooplankton abundances, lower concentrations of suspended matter, weaker particle fluxes and weaker attenuation rates (Fig. 3B) and with stronger attenuation rates of organisms' abundances (Fig. 3A). Therefore, we propose that oligotrophic regimes feature a network of diverse taxa that is not efficient at using the low amount of material fluxing. Our results are consistent with previous studies suggesting that those oligotrophic regimes can be relatively efficient at exporting the slow-sinking fraction of the little carbon that is produced in the surface layers due to a low impact of zooplankton grazing on the sinking particles (Guidi et al., 2009; Henson et al., 2015). This regime could help explain why we found the lowest particle flux attenuation rates in the tropics.

Global vertical patterns of zooplankton and particle flux

The concentration and biomass of various zooplankton groups decreased with depth (Fig. S1), confirming the general trend of decreasing zooplankton abundance and biomass from the surface to 1000 m depth (Bode et al., 2018; Brugnano et al., 2012; Hernández-León et al., 2020; Koppelmann et al., 2005; Kosobokova and Hopcroft, 2010; Yamaguchi et al., 2004). Among these earlier studies, two models for the attenuation of zooplankton have been proposed: an exponential or a power model. Here, we used the power model (equation 1) because it was widely used to model vertical flux attenuation rates (Martin et al., 1987). Based on this power model, we observed rates of decrease in zooplankton abundance or biomass (Fig. 3) that were in the same range as those reported in the western Pacific Ocean (-1.52 to -1.41 for abundance and -1.32 to -1.10 for biomass, (Yamaguchi et al., 2002). Zooplankton abundance decreased more rapidly with depth than biomass as the average size of organisms increased with depth, confirming that the contribution of larger species increases with depth (Homma and Yamaguchi, 2010; Yamaguchi et al., 2002). Considering a larger latitudinal band than earlier studies who found weak regional or global patterns (Hernández-León et al., 2020; Puelles et al., 2019), we showed that the rates of zooplankton attenuation vary with latitude and to a lesser extent with oxygen concentrations (Fig. 3) and also in the opposite direction of the flux attenuation.

Stronger surface particle fluxes and vertical attenuation rates were found at higher latitudes where primary production is mainly ensured by the microphytoplankton and weaker flux and attenuation was found in the low latitude dominated by picophytoplankton (Fig.4). Such latitudinal pattern in particle attenuation rates results from the gradient in the production regime and has been observed quasi-systematically with imaging systems on global scales

(Guidi et al., 2015), but also based on sediment traps (Berelson, 2001) or combining sediment traps with satellite-based estimates of primary production (Henson et al., 2012). However, several short-term experiments at selected sites from temperate to tropical latitudes of the Pacific and Atlantic, showed an opposite pattern with stronger flux and attenuation in cold and productive regions compared to inter-tropical oligotrophic (Buesseler et al., 2007; Marsay et al., 2015). The inconsistency of the observations is difficult to explain although it was noted that depth varying remineralisation due to varying temperature may reconcile the contrasted results (Marsay et al., 2015). It is possible that some of the variations arise from the use of different methodologies (instruments, time scale, global representation of the dataset) to address the complexity of the processes to be measured simultaneously.

Opposite pattern between the vertical attenuations of zooplankton abundance (A_Zoo) and biomass (B_zoo) in one hand and the vertical attenuation of flux (A_Flux) in the other hand supports the view that the abundant zooplankton community plays a crucial role in flux attenuation in productive layers, by feeding and fragmenting the sinking material as suggested in previous studies (Dilling and Alldredge, 2000; Giering et al., 2014; Lampitt et al., 1990; Stemmann et al., 2004). However, on average and more importantly at high latitudes, zooplankton attenuation rates were stronger than the vertical flux attenuation rates (Fig. 3) indicating that zooplankton vertical zonation may be affected by other processes than the resources provided by the flux of organic matter from the epipelagic layer. In the inter-tropical OMZ regions, zooplankton vertical attenuation rates were maximum when the vertical attenuation of the particle's flux was minimum. Previous studies have reported lower flux attenuation rates in the OMZ of the Arabian Sea (Haake et al., 1992; Roullier et al., 2014), and Eastern Tropical North Pacific (Cavan et al., 2017; Van Mooy et al., 2002). Lower zooplankton activity together with reduced bacterial activity (Cram et al., 2021) allow sinking particles to transit through the OMZ core without being severely degraded (Wishner et al., 2008, 1995) .

Sensitivity of plankton and vertical flux to varying oxygen conditions

By comparing zooplankton communities from inter-tropical stations with those from oxygenated mesopelagic layers to stations from OMZs, our analysis brought additional evidence that change in zooplankton community composition may affect the efficiency of the BCP. The zooplankton community sampled in the Indian Ocean OMZ displayed a distinct composition compared to the other samples, which is in line with the increasing number of

studies that document the profound impact of oxygen depletion on pelagic organisms (Ekau et al., 2010; Hauss et al., 2016; Wishner et al., 2018). Our results underlined how the OMZ can strongly reduce the abundance of several zooplankton groups (i.e. Calanoida, Euphausiacea, Amphipoda, Ostracoda) that are outcompeted by more hypoxia-tolerant ones. We found that tunicates (mostly Appendicularia), large protists (Collodaria and Foraminifera), polychaetes, Oncaeidae, Oithinidae and to a lesser extent Cnidaria (jellyfishes) may tolerate OMZ conditions, since their abundance at OMZ and at non-OMZ stations did not present significant differences. All of these zooplankton groups have been reported as being able to thrive or endure at low oxygen concentrations in various OMZs (Ekau et al., 2010; Hauss et al., 2016; Keister and Tuttle, 2013; Kiko and Hauss, 2019; Parris et al., 2014; Tutasi and Escribano, 2020; Werner and Buchholz, 2013; Wishner et al., 2020). Those "hypoxiphilic" or hypoxia-tolerant taxa display special adaptations that enable them to remain at extremely low oxygen concentrations where other zooplankton groups cannot, because they fail to meet their metabolic oxygen demand (Childress and Seibel, 1998; Seibel, 2011). Jellyfish and large protists benefit from their passive feeding tactics which are less oxygen-demanding than active cruising and filter feeding (Kiørboe, 2011). Indeed, hypoxia-tolerant taxa can also display behavioral adaptations that cut down the metabolic costs associated with active feeding or the active search for mates in the water column. Copepod species belonging to the Oncaeidae and Oithonidae families are known for performing ambush feeding tactics or to attach themselves on large detritus (Brun et al., 2017), which allows them to capture small preys or to feed on falling detritus at very low metabolic costs. Therefore, these less motile copepods frequently outcompete most of their calanoid congeners in OMZs and often co-occur with Appendicularia, as those discard particle-rich aggregates on which the copepods feed (Alldredge, 1972; Brun et al., 2017; Kiørboe, 2011). Other possible adaptations consist in the use of lipid storages and metabolic suppression (Wishner et al., 2020).

Some organisms conduct diapause in the OMZ for an extended period, allowing them to avoid foraging predators and to complete their life cycle (Arashkevich et al., 1996). Diapause reduces energetic costs and thus allows the organisms to survive in resource-depleted conditions. Metabolic suppression goes hand in hand with the diapause, but can also occur on shorter time scales, e.g. when organisms stay at OMZ depth during diel vertical migrations. Diapause and metabolic suppression are associated with reduced respiratory and locomotor activity. Feeding on and disruption of particles could therefore be reduced at OMZ depth not only due to the exclusion of many hypoxia intolerant zooplankton organisms, but also due to the reduced activity of those zooplankton organisms that can cope with OMZ

conditions. The zooplankton groups we found to characterize the community inhabiting the hypoxic and anoxic layers are those that commonly outcompete others in OMZs worldwide. They could benefit from the likely future expansion of OMZ (Oschlies et al., 2018) and thus become increasingly abundant with future climate change. Such changes could probably result in enhanced vertical particle flux in those regions. However, this requires further research as some of these organisms could already be living near their physiological hypoxia tolerance limits (Wishner et al., 2018).

Conclusions

We showed that consistent observations can be obtained at a global level using *in situ* camera systems and precise net sampling in various ecosystems representative of different ocean conditions. In future surveys, consistently combining these techniques with acoustic and other bio-optical sensors will allow the measurement of the vertical and horizontal distribution of organisms with greater precision. We showed that the key environmental variables driving epipelagic mesozooplankton community structure at the global scale are temperature, phytoplankton biomass and key groups/size. In the mesopelagic layer, surface phytoplankton size classes, particle concentration, temperature and oxygen availability were identified as the main drivers of mesozooplankton community structure. Our work furthermore suggests that low attenuation of zooplankton abundance and biomass go in hand with high particle flux attenuation and vice versa. Such information is crucial for the parameterization of marine ecosystem models that describe complex zooplankton-related processes based on coarse but increasingly numerous functional types. These models suggest that surface phytoplankton biomass and size classes, the flux of particles and the oxygen content in the mesopelagic layer will all be affected further by global climate change. The fact that zooplankton communities are sensitive to those factors suggests that future climatic changes may profoundly alter zooplankton communities worldwide, at the surface but also in the deeper mesopelagic layer.

ACKNOWLEDGMENTS

We thank the reviewers for their comments which help to improve the manuscript. Tara Oceans (which includes both the Tara Oceans and Tara Oceans Polar Circle expeditions) would not exist without the leadership of the Tara Ocean Foundation and the continuous support of 23 institutes (https://oceans.taraexpeditions.org/). This study has received the

number 123. This study is part of the “Ocean Plankton, Climate and Development” project funded by the French Facility for Global Environment (FFEM). Y.D.S. and M.C.B. received financial support from FFEM to execute the project. R.K acknowledges support via a “Make Our Planet Great Again” grant of the French National Research Agency within the “Programme d’Investissements d’Avenir”; reference “ANR-19-MPGA-0012”. F.B. received support from ETH Zürich. L.S. received funding from the Chair Vision at Sorbonne University. This project has received funding from the European Union’s Horizon 2020 research and innovation programme under grant agreement No 862923. This output reflects only the author’s view, and the European Union cannot be held responsible for any use that may be made of the information contained therein. We further thank the commitment of the following sponsors: CNRS (in particular Groupement de Recherche GDR3280 and the Research Federation for the Study of Global Ocean Systems Ecology and Evolution FR2022/Tara Oceans-GOSEE), the European Molecular Biology Laboratory (EMBL), the French Ministry of Research, and the French Government ‘‘Investissements d’Avenir’’ programs OCEANOMICS (ANR-11-BTBR-0008), the EMBRC-France (ANR-10-INBS-02). Funding for the collection and processing of the Tara Oceans data set was provided by NASA Ocean Biology and Biogeochemistry Program under grants NNX11AQ14G, NNX09AU43G, NNX13AE58G, and NNX15AC08G (to the University of Maine); the Canada Excellence research chair on remote sensing of Canada’s new Arctic frontier; and the Canada Foundation for Innovation. We also thank Agnès b. and Etienne Bourgois, the Prince Albert II de Monaco Foundation, the Veolia Foundation, Region Bretagne, Lorient Agglomeration, Serge Ferrari, Worldcourier, and KAUST for support and commitment. The global sampling effort was enabled by countless scientists and crew who sampled aboard the Tara from 2009–2013, and we thank MERCATOR-CORIOLIS and ACRI-ST for providing daily satellite data during the expeditions. We are also grateful to the countries who graciously granted sampling permission.

References

Alldredge, A.L., 1972. Abandoned larvacean houses : a unique food source in pelagic environment. Science 177, 885.

Andersen, V., Francois, F., Sardou, J., Picheral, M., Scotto, M., Nival, P., 1998. Vertical distributions of macroplankton and micronekton in the Ligurian and Tyrrhenian Seas (northwestern Mediterranean). Oceanologica Acta 21, 655–676.

Arashkevich, E., Drits, A., Timonin, A., 1996. Diapause in the life cycle of Calanoides carinatus (Kroyer),(Copepoda, Calanoida). Hydrobiologia 320, 197–208.

Balazy, K., Trudnowska, E., Wichorowski, M., Błachowiak-Samołyk, K., 2018. Large versus small zooplankton in relation to temperature in the Arctic shelf region. Polar Research 37, 1427409.

Banse, K., 1964. On the vertical distribution of zooplankton in the sea. Progress in oceanography 2, 53–125.

Beaugrand, G., Conversi, A., Atkinson, A., Cloern, J., Chiba, S., Fonda-Umani, S., Kirby, R.R., Greene, C.H., Goberville, E., Otto, S.A., Reid, P.C., Stemmann, L., Edwards, M., 2019. Prediction of unprecedented biological shifts in the global ocean. Nature Climate Change 9, 237-+. https://doi.org/10.1038/s41558-019-0420-1

Berelson, W.M., 2002. Particle settling rates increase with depth in the ocean. Deep-Sea Research Part Ii-Topical Studies in Oceanography 49, 237–251.

Berelson, W.M., 2001. The Flux of Particulate Organic Carbon Into the Ocean Interior: A Comparison of Four U.S. JGOFS Regional Studies. Oceanography 14, 59–67.

Biard, T., Stemmann, L., Picheral, M., Mayot, N., Vandromme, P., Hauss, H., Gorsky, G., Guidi, L., Kiko, R., Not, F., 2016. In situ imaging reveals the biomass of giant protists in the global ocean. Nature 532, 504-+. https://doi.org/10.1038/nature17652

Bode, M., Hagen, W., Cornils, A., Kaiser, P., Auel, H., 2018. Copepod distribution and biodiversity patterns from the surface to the deep sea along a latitudinal transect in the eastern Atlantic Ocean (24°N to 21°S). Progress in Oceanography 161, 66–77. https://doi.org/10.1016/j.pocean.2018.01.010

Böttger-Schnack, R., 1996. Vertical structure of small metazoan plankton, especially noncalanoid copepods. I. Deep Arabian Sea. Journal of Plankton Research 18, 1073–1101. https://doi.org/10.1093/plankt/18.7.1073

Brugnano, C., Granata, A., Guglielmo, L., Zagami, G., 2012. Spring diel vertical distribution of copepod abundances and diversity in the open Central Tyrrhenian Sea (Western Mediterranean). Journal of Marine Systems 105, 207–220.

Brun, P., Payne, M.R., Kiørboe, T., 2017. A trait database for marine copepods. Earth System Science Data 9, 99–113.

Buesseler, K.O., Lamborg, C.H., Boyd, P.W., Lam, P.J., Trull, T.W., Bidigare, R.R., Bishop, J.K.B., Casciotti, K.L., Dehairs, F., Elskens, M., Honda, M., Karl, D.M., Siegel, D.A., Silver, M.W., Steinberg, D.K., Valdes, J., Van Mooy, B., Wilson, S., 2007. Revisiting Carbon Flux Through the Ocean's Twilight Zone. Science 316, 567–570. https://doi.org/10.1126/science.1137959

Cavan, E.L., Henson, S.A., Belcher, A., Sanders, R., 2017. Role of zooplankton in determining

the efficiency of the biological carbon pump. Biogeosciences 14, 177–186.

Childress, J.J., Seibel, B.A., 1998. Life at stable low oxygen levels: adaptations of animals to oceanic oxygen minimum layers. The Journal of experimental biology 201, 1223–1232.

Chust, G., Allen, J.I., Bopp, L., Schrum, C., Holt, J., Tsiaras, K., Zavatarelli, M., Chifflet, M., Cannaby, H., Dadou, I., 2014. Biomass changes and trophic amplification of plankton in a warmer ocean. Global Change Biology 20, 2124–2139.

Coma, R., Ribes, M., Serrano, E., Jiménez, E., Salat, J., Pascual, J., 2009. Global warming-enhanced stratification and mass mortality events in the Mediterranean. Proceedings of the National Academy of Sciences 106, 6176–6181.

Cram, J., Fuchsman, C., Duffy, M., Pretty, J., Lekanoff, R., Neibauer, J., Leung, S., Huebert, K.B., Weber, T., Bianchi, D., 2021. Slow particle remineralization, rather than suppressed disaggregation, drives efficient flux transfer through the Eastern Tropical North Pacific Oxygen Deficient Zone. Earth and Space Science Open Archive ESSOAr.

Dilling, L., Alldredge, A.L., 2000. Fragmentation of marine snow by swimming macrozooplankton: A new process impacting carbon cycling in the sea. Deep-Sea Research Part I-Oceanographic Research Papers 47, 1227–1245.

Ekau, W., Auel, H., Portner, H.O., Gilbert, D., 2010. Impacts of hypoxia on the structure and processes in pelagic communities (zooplankton, macro-invertebrates and fish). Biogeosciences 7, 1669–1699. https://doi.org/10.5194/bg-7-1669-2010

Everett, J.D., Baird, M.E., Buchanan, P., Bulman, C., Davies, C., Downie, R., Griffiths, C., Heneghan, R., Kloser, R.J., Laiolo, L., 2017. Modeling what we sample and sampling what we model: challenges for zooplankton model assessment. Frontiers in Marine Science 4, 77.

Fernández de Puelles, M., Gazá, M., Cabanellas-Reboredo, M., Santandreu, M., Irigoien, X., González-Gordillo, J.I., Duarte, C.M., Hernández-León, S., 2019. Zooplankton abundance and diversity in the tropical and subtropical ocean. Diversity 11, 203.

Forest, A., Babin, M., Stemmann, L., Picheral, M., Sampei, M., Fortier, L., Gratton, Y., Belanger, S., Devred, E., Sahlin, J., Doxaran, D., Joux, F., Ortega-Retuerta, E., Martin, J., Jeffrey, W.H., Gasser, B., Miquel, J.C., 2013. Ecosystem function and particle flux dynamics across the Mackenzie Shelf (Beaufort Sea, Arctic Ocean): an integrative analysis of spatial variability and biophysical forcings. Biogeosciences 10, 2833–2866. https://doi.org/10.5194/bg-10-2833-2013

Gaard, E., Gislason, A., Falkenhaug, T., Søiland, H., Musaeva, E., Vereshchaka, A., Vinogradov, G., 2008. Horizontal and vertical copepod distribution and abundance on the Mid-Atlantic Ridge in June 2004. Deep Sea Research Part II: topical studies in oceanography 55, 59–71.

Gallienne, C.P., Robins, D.B., Woodd-Walker, R.S., 2001. Abundance, distribution and size structure of zooplankton along a 20 degrees west meridional transect of the northeast Atlantic Ocean in July. Deep-Sea Research Part Ii-Topical Studies in Oceanography 48, 925–949.

Gehlen, M., Bopp, L., Ernprin, N., Aumont, O., Heinze, C., Raguencau, O., 2006. Reconciling surface ocean productivity, export fluxes and sediment composition in a global biogeochemical ocean model. Biogeosciences 3, 521–537.

Giering, S.L.C., Richard Sanders, Richard S. Lampitt, Thomas R. Anderson, Christian Tamburini, Mehdi Boutrif, Mikhail V. Zubkov, Chris M. Marsay, Stephanie A. Henson, Kevin Saw, Kathryn Cook, Daniel J. Mayor, 2014. Reconciliation of the carbon budget in the ocean's twilight zone. Nature 507, 17. https://doi.org/10.1038/nature13123

751 Gorsky, G., Ohman, M.D., Picheral, M., Gasparini, S., Stemmann, L., Romagnan, J.-B.,
752 Cawood, A., Pesant, S., Garcia-Comas, C., Prejger, F., 2010. Digital zooplankton image
753 analysis using the ZooScan integrated system. Journal of Plankton Research 32, 285–303.
754 https://doi.org/10.1093/plankt/fbp124

755 Guidi, L., Chaffron, S., Bittner, L., Eveillard, D., Larhlimi, A., Roux, S., Darzi, Y., Audic, S.,
756 Berline, L., Brum, J.R., Coelho, L.P., Espinoza, J.C.I., Malviya, S., Sunagawa, S., Dimier, C.,
757 Kandels-Lewis, S., Picheral, M., Poulain, J., Searson, S., Stemmann, L., Not, F., Hingamp, P.,
758 Speich, S., Follows, M., Karp-Boss, L., Boss, E., Ogata, H., Pesant, S., Weissenbach, J.,
759 Wincker, P., Acinas, S.G., Bork, P., de Vargas, C., Iudicone, D., Sullivan, M.B., Raes, J.,
760 Karsenti, E., Bowler, C., Gorsky, G., Tara Oceans Consortium Coordinator, 2016. Plankton
761 networks driving carbon export in the oligotrophic ocean. Nature 532, 465-+.

762 Guidi, L., Jackson, G.A., Stemmann, L., Miquel, J.C., Picheral, M., Gorsky, G., 2008.
763 Relationship between particle size distribution and flux in the mesopelagic zone. Deep-Sea
764 Research Part I-Oceanographic Research Papers 55, 1364–1374.

765 Guidi, L., Legendre, L., Reygondeau, G., Uitz, J., Stemmann, L., Henson, S.A., 2015. A new
766 look at ocean carbon remineralization for estimating deepwater sequestration. Global
767 Biogeochem. Cycles 29, 1044–1059. https://doi.org/10.1002/2014gb005063

768 Guidi, L., Stemmann, L., Jackson, G.A., Ibanez, F., Claustre, H., Legendre, L., Picheral, M.,
769 Gorsky, G., 2009. Effects of phytoplankton community on production, size and export of
770 large aggregates: A world-ocean analysis. Limnology and Oceanography 54, 1951–1963.
771 https://doi.org/10.4319/lo.2009.54.6.1951

772 Haake, B., Ittekkot, V., Ramaswamy, V., Nair, R., Honjo, S., 1992. Fluxes of amino acids and
773 hexosamines to the deep Arabian Sea. Marine Chemistry 40, 291–314.

774 Hauss, H., Christiansen, S., Schütte, F., Kiko, R., Edvam Lima, M., Rodrigues, E., Karstensen,
775 J., Löscher, C.R., Körtzinger, A., Fiedler, B., 2016. Dead zone or oasis in the open ocean?
776 Zooplankton distribution and migration in low-oxygen modewater eddies. Biogeosciences 13,
777 1977–1989.

778 Henson, S.A., Sanders, R., Madsen, E., 2012. Global patterns in efficiency of particulate organic
779 carbon export and transfer to the deep ocean. Global Biogeochemical Cycles 26.

780 Henson, S.A., Yool, A., Sanders, R., 2015. Variability in efficiency of particulate organic carbon
781 export: A model study. Global Biogeochemical Cycles 29, 33–45.

782 Hernández-León, S., Koppelmann, R., Fraile-Nuez, E., Bode, A., Mompeán, C., Irigoien, X.,
783 Olivar, M.P., Echevarría, F., de Puelles, M.F., González-Gordillo, J.I., 2020. Large deep-sea
784 zooplankton biomass mirrors primary production in the global ocean. Nature communications
785 11, 1–8.

786 Hidalgo, P., Escribano, R., Fuentes, M., Jorquera, E., Vergara, O., 2012. How coastal upwelling
787 influences spatial patterns of size-structured diversity of copepods off central-southern Chile
788 (summer 2009). Progress in Oceanography 92, 134–145.

789 Hirche, H.-J., Mumm, N., 1992. Distribution of dominant copepods in the Nansen Basin, Arctic
790 Ocean, in summer. Deep Sea Research Part A. Oceanographic Research Papers 39, S485–
791 S505.

792 Homma, T., Yamaguchi, A., 2010. Vertical changes in abundance, biomass and community
793 structure of copepods down to 3000 m in the southern Bering Sea. Deep Sea Research Part I:
794 Oceanographic Research Papers 57, 965–977.

795 Ibarbalz, F.M., Henry, N., Brandao, M.C., Martini, V., Busseni, G., Byrne, H., Coelho, L.P.,

796 Endo, H., Gasol, J.M., Gregory, A.C., Mahe, F., Rigonato, J., Royo-Llonch, M., Salazar, G.,
797 Sanz-Saez, I., Scalco, E., Soviadan, D., Zayed, A.A., Zingone, A., Labadie, K., Ferland, J.,
798 Marec, C., Kandels, S., Picheral, M., Dimier, C., Poulain, J., Pisarev, S., Carmichael, M.,
799 Pesant, S., Acinas, S.G., Babin, M., Bork, P., Boss, E., Bowler, C., Cochrane, G., de Vargas,
800 C., Follows, M., Gorsky, G., Grimsley, N., Guidi, L., Hingamp, P., Iudicone, D., Jaillon, O.,
801 Kandels, S., Karp-Boss, L., Karsenti, E., Not, F., Ogata, H., Pesant, S., Poulton, N., Raes, J.,
802 Sardet, C., Speich, S., Stemmann, L., Sullivan, M.B., Sunagawa, S., Wincker, P., Bopp, L.,
803 Lombard, F., Zinger, L., Tara Oceans, C., 2019. Global Trends in Marine Plankton Diversity
804 across Kingdoms of Life. Cell 179, 1084-+. https://doi.org/10.1016/j.cell.2019.10.008

805 Irigoien, X., Klevjer, T.A., Røstad, A., Martinez, U., Boyra, G., Acuña, J.L., Bode, A.,
806 Echevarria, F., Gonzalez-Gordillo, J.I., Hernandez-Leon, S., 2014. Large mesopelagic fishes
807 biomass and trophic efficiency in the open ocean. Nature communications 5, 1–10.

808 Iversen, M.H., Lampitt, R.S., 2020. Size does not matter after all: no evidence for a size-sinking
809 relationship for marine snow. Progress in Oceanography 189, 102445.

810 Karsenti, E., Acinas, S.G., Bork, P., Bowler, C., De Vargas, C., Raes, J., Sullivan, M., Arendt,
811 D., Benzoni, F., Claverie, J.M., Follows, M., Gorsky, G., Hingamp, P., Iudicone, D., Jaillon,
812 O., Kandels-Lewis, S., Krzic, U., Not, F., Ogata, H., Pesant, S., Reynaud, E.G., Sardet, C.,
813 Sieracki, M.E., Speich, S., Velayoudon, D., Weissenbach, J., Wincker, P., Tara Oceans, C.,
814 2011. A Holistic Approach to Marine Eco-Systems Biology. Plos Biology 9.
815 https://doi.org/e1001177 10.1371/journal.pbio.1001177

816 Keister, J.E., Tuttle, L.B., 2013. Effects of bottom-layer hypoxia on spatial distributions and
817 community structure of mesozooplankton in a sub-estuary of Puget Sound, Washington, USA.
818 Limnology and Oceanography 58, 667–680.

819 Kiko, R., Biastoch, A., Brandt, P., Cravatte, S., Hauss, H., Hummels, R., Kriest, I., Marin, F.,
820 McDonnell, A.M.P., Oschlies, A., Picheral, M., Schwarzkopf, F.U., Thurnherr, A.M.,
821 Stemmann, L., 2017. Biological and physical influences on marine snowfall at the equator.
822 Nature Geoscience 10, 852-+. https://doi.org/10.1038/ngeo3042

823 Kiko, R., Brandt, P., Christiansen, S., Faustmann, J., Kriest, I., Rodrigues, E., Schütte, F., Hauss,
824 H., 2020. Zooplankton-mediated fluxes in the eastern tropical North Atlantic. Frontiers in
825 Marine Science 1.

826 Kiko, R., Hauss, H., 2019. On the estimation of zooplankton-mediated active fluxes in oxygen
827 minimum zone regions. Frontiers in Marine Science 6, 741.

828 Kiørboe, T., 2013. Zooplankton body composition. Limnology and Oceanography 58, 1843–
829 1850.

830 Kiørboe, T., 2011. What makes pelagic copepods so successful? Journal of Plankton Research
831 33, 677–685.

832 Kiørboe, T., Visser, A., Andersen, K.H., Handling editor: Howard Browman, 2018. A trait-based
833 approach to ocean ecology. ICES Journal of Marine Science.
834 https://doi.org/10.1093/icesjms/fsy090

835 Koppelmann, R., Weikert, H., Halsband-Lenk, C., Jennerjahn, T., 2004. Mesozooplankton
836 community respiration and its relation to particle flux in the oligotrophic eastern
837 Mediterranean. Global Biogeochemical Cycles 18.

838 Koppelmann, R., Zimmermann-Timm, H., Weikert, H., 2005. Bacterial and zooplankton
839 distribution in deep waters of the Arabian Sea. Deep-Sea Research Part I-Oceanographic
840 Research Papers 52, 2184–2192. https://doi.org/10.1016/j.dsr.2005.06.012

841 Kosobokova, K.N., Hopcroft, R.R., 2010. Diversity and vertical distribution of mesozooplankton
842 in the Arctic's Canada Basin. Deep Sea Research Part II: Topical Studies in Oceanography
843 57, 96–110.

844 Kwiatkowski, L., Aumont, O., Bopp, L., 2019. Consistent trophic amplification of marine
845 biomass declines under climate change. Global change biology 25, 218–229.

846 Lampitt, R.S., Noji, T., Von Bodungen, B., 1990. What happens to zooplankton fecal pellets ?
847 Implication for material flux. Marine Biology 104, 15–23.

848 Laws, R.M., 1985. The ecology of the Southern Ocean. Amer. Scient. 73, 26–40.

849 Legendre, P., Legendre, L., 1998. Numerical ecology, 2nd english. ed, Developments in
850 environmental modelling 20. Elsevier, Amsterdam.

851 Lehette, P., Hernandez-Leon, S., 2009. Zooplankton biomass estimation from digitized images: a
852 comparison between subtropical and Antarctic organisms. Limnology and Oceanography-
853 Methods 7, 304–308.

854 Madhupratap, M., Nair, KNV, Venugopal, P., Gauns, M., Haridas, P., Gopalakrishnan, T., Nair,
855 KKC, 2004. Arabian Sea oceanography and fisheries.

856 Marsay, C.M., Sanders, R.J., Henson, S.A., Pabortsava, K., Achterberg, E.P., Lampitt, R.S.,
857 2015. Attenuation of sinking particulate organic carbon flux through the mesopelagic ocean.
858 Proceedings of the National Academy of Sciences 112, 1089–1094.

859 Martin, J.H., Knauer, G.A., Karl, D.M., Broenkow, W.W., 1987. VERTEX: Carbon cycling in
860 the Northeast Pacific. Deep-Sea Research 34, 267–285.

861 Morrison, J.M., Codispoti, L., Smith, S.L., Wishner, K., Flagg, C., Gardner, W.D., Gaurin, S.,
862 Naqvi, S., Manghnani, V., Prosperie, L., 1999. The oxygen minimum zone in the Arabian Sea
863 during 1995. Deep Sea Research Part II: Topical Studies in Oceanography 46, 1903–1931.

864 MOTODA, S., 1959. Devices of simple plankton apparatus. Memoirs of the faculty of fisheries
865 Hokkaido University 7, 73–94.

866 Ohman, M.D., Romagnan, J.B., 2016. Nonlinear effects of body size and optical attenuation on
867 Diel Vertical Migration by zooplankton. Limnology and Oceanography 61, 765–770.
868 https://doi.org/10.1002/lno.10251

869 Oschlies, A., Brandt, P., Stramma, L., Schmidtko, S., 2018. Drivers and mechanisms of ocean
870 deoxygenation. Nature Geoscience 11, 467–473.

871 Paffenhofer, G.A., Mazzocchi, M.G., 2003. Vertical distribution of subtropical epiplanktonic
872 copepods. Journal of Plankton Research 25, 1139–1156.

873 Palomares-García, R.J., Gómez-Gutiérrez, J., Robinson, C.J., 2013. Winter and summer vertical
874 distribution of epipelagic copepods in the Gulf of California. Journal of Plankton Research
875 35, 1009–1026.

876 Park, C., Wormuth, J., 1993. Distribution of Antarctic zooplankton around Elephant Island
877 during the austral summers of 1988, 1989, and 1990. Polar Biology 13, 215–225.

878 Parris, D.J., Ganesh, S., Edgcomb, V.P., DeLong, E.F., Stewart, F.J., 2014. Microbial eukaryote
879 diversity in the marine oxygen minimum zone off northern Chile. Frontiers in microbiology 5,
880 543.

881 Pesant, S., Not, F., Picheral, M., Kandels-Lewis, S., Le Bescot, N., Gorsky, G., Iudicone, D.,
882 Karsenti, E., Speich, S., Trouble, R., Dimier, C., Searson, S., Tara Oceans Consortium, C.,
883 2015. Open science resources for the discovery and analysis of Tara Oceans data. Scientific

884 data 2, 150023–150023. https://doi.org/10.1038/sdata.2015.23

885 Picheral, M., Guidi, L., Stemmann, L., Karl, D.M., Iddaoud, G., Gorsky, G., 2010. The
886 Underwater Vision Profiler 5: An advanced instrument for high spatial resolution studies of
887 particle size spectra and zooplankton. Limnology and Oceanography-Methods 8, 462–473.
888 https://doi.org/10.4319/lom.2010.8.462

889 Pinkerton, M.H., Décima, M., Kitchener, J.A., Takahashi, K.T., Robinson, K.V., Stewart, R.,
890 Hosie, G.W., 2020. Zooplankton in the Southern Ocean from the continuous plankton
891 recorder: Distributions and long-term change. Deep Sea Research Part I: Oceanographic
892 Research Papers 162, 103303.

893 Quetin, L.B., Ross, R.M., Frazer, T.K., Haberman, K.L., 1996. Factors affecting distribution and
894 abundance of zooplankton, with an emphasis on Antarctic krill, Euphausia superba. Antarctic
895 Research Series 70, 357–371.

896 Remsen, A., Hopkins, T.L., Samson, S., 2004. What you see is not what you catch: a comparison
897 of concurrently collected net, Optical Plankton Counter, and Shadowed Image Particle
898 Profiling Evaluation Recorder data from the northeast Gulf of Mexico. Deep-Sea Research
899 Part I-Oceanographic Research Papers 51, 129–151.

900 Richardson, A.J., 2008. In hot water: zooplankton and climate change. ICES Journal of Marine
901 Science 65, 279–295. https://doi.org/10.1093/icesjms/fsn028

902 Robinson, C., Steinberg, D.K., Anderson, T.R., Aristegui, J., Carlson, C.A., Frost, J.R.,
903 Ghiglione, J.F., Hernandez-Leon, S., Jackson, G.A., Koppelmann, R., Queguiner, B.,
904 Ragueneau, O., Rassoulzadegan, F., Robison, B.H., Tamburini, C., Tanaka, T., Wishner, K.F.,
905 Zhang, J., 2010. Mesopelagic zone ecology and biogeochemistry - a synthesis. Deep-Sea
906 Research Part Ii-Topical Studies in Oceanography 57, 1504–1518.
907 https://doi.org/10.1016/j.dsr2.2010.02.018

908 Roe, H., 1988. Midwater biomass profiles over the Madeira Abyssal Plain and the contribution
909 of copepods, in: Biology of Copepods. Springer, pp. 169–181.

910 Rombouts, I., Beaugrand, G., Ibanez, F., Gasparini, S., Chiba, S., Legendre, L., 2010. A
911 multivariate approach to large-scale variation in marine planktonic copepod diversity and its
912 environmental correlates. Limnology and Oceanography 55, 2219–2229.
913 https://doi.org/10.4319/lo.2010.55.5.2219

914 Ross, R.M., Quetin, L.B., Martinson, D.G., Iannuzzi, R.A., Stammerjohn, S.E., Smith, R.C.,
915 2008. Palmer LTER: Patterns of distribution of five dominant zooplankton species in the
916 epipelagic zone west of the Antarctic Peninsula, 1993–2004. Deep Sea Research Part II:
917 Topical Studies in Oceanography 55, 2086–2105.

918 Roullier, F., Berline, L., Guidi, L., De Madron, X.D., Picheral, M., Sciandra, A., Pesant, S.,
919 Stemmann, L., 2014. Particle size distribution and estimated carbon flux across the Arabian
920 Sea oxygen minimum zone. Biogeosciences 11, 4541–4557. https://doi.org/10.5194/bg-11-
921 4541-2014

922 Rutherford, S., D'Hondt, S., Prell, W., 1999. Environmental controls on the geographic
923 distribution of zooplankton diversity. Nature 400, 749–753. https://doi.org/10.1038/23449

924 Saporiti, F., Bearhop, S., Vales, D.G., Silva, L., Zenteno, L., Tavares, M., Crespo, E.A.,
925 Cardona, L., 2015. Latitudinal changes in the structure of marine food webs in the
926 Southwestern Atlantic Ocean. Marine Ecology Progress Series 538, 23–34.

927 Schmidtko, S., Stramma, L., Visbeck, M., 2017. Decline in global oceanic oxygen content during
928 the past five decades. Nature 542, 335–339.

929 Seibel, B.A., 2011. Critical oxygen levels and metabolic suppression in oceanic oxygen
930 minimum zones. Journal of Experimental Biology 214, 326–336.

931 Smith, S., Roman, M., Prusova, I., Wishner, K., Gowing, M., Codispoti, L.A., Barber, R., Marra,
932 J., Flagg, C., 1998. Seasonal response of zooplankton to monsoonal reversals in the Arabian
933 Sea. Deep-Sea Research Part II 45, 2369–2403.

934 St John, M.A., Borja, A., Chust, G., Heath, M., Grigorov, I., Mariani, P., Martin, A.P., Santos,
935 R.S., 2016. A dark hole in our understanding of marine ecosystems and their services:
936 perspectives from the mesopelagic community. Frontiers in Marine Science 3, 31.

937 Steinberg, D.K., Landry, M.R., 2017. Zooplankton and the ocean carbon cycle. Annual review of
938 marine science 9, 413–444.

939 Steinberg, D.K., Ruck, K.E., Gleiber, M.R., Garzio, L.M., Cope, J.S., Bernard, K.S.,
940 Stammerjohn, S.E., Schofield, O.M., Quetin, L.B., Ross, R.M., 2015. Long-term (1993–2013)
941 changes in macrozooplankton off the Western Antarctic Peninsula. Deep Sea Research Part I:
942 Oceanographic Research Papers 101, 54–70.

943 Stemmann, L., Jackson, G.A., Gorsky, G., 2004. A vertical model of particle size distributions
944 and fluxes in the midwater column that includes biological and physical processes - Part II:
945 application to a three year survey in the NW Mediterranean Sea. Deep-Sea Research Part I-
946 Oceanographic Research Papers 51, 885–908. https://doi.org/10.1016/j.dsr.2004.03.002

947 Stempniewicz, L., Błachowiak-Samołyk, K., Węsławski, J.M., 2007. Impact of climate change
948 on zooplankton communities, seabird populations and arctic terrestrial ecosystem—a
949 scenario. Deep Sea Research Part II: Topical Studies in Oceanography 54, 2934–2945.

950 Stramma, L., Schmidtko, S., Levin, L.A., Johnson, G.C., 2010. Ocean oxygen minima
951 expansions and their biological impacts. Deep Sea Research Part I: Oceanographic Research
952 Papers 57, 587–595. https://doi.org/10.1016/j.dsr.2010.01.005

953 Stukel, M.R., Ohman, M.D., Kelly, T.B., Biard, T., 2019. The roles of suspension-feeding and
954 flux-feeding zooplankton as gatekeepers of particle flux into the mesopelagic ocean in the
955 Northeast Pacific. Frontiers in Marine Science 6, 397.

956 Tarling, G.A., Shreeve, R.S., Ward, P., Atkinson, A., Hirst, A.G., 2004. Life-cycle phenotypic
957 composition and mortality of Calanoides acutus (Copepoda : Calanoida) in the Scotia Sea: a
958 modelling approach. Marine Ecology-Progress Series 272, 165–181.

959 Terazaki, M., Wada, M., 1988. Occurrence of large numbers of carcasses of the large, grazing
960 copepod Calanus cristatus from the Japan Sea. Marine Biology 97, 177–183.

961 Trudnowska, E., Lacour, L., Ardyna, M., Rogge, A., Irisson, J.O., Waite, A.M., Babin, M.,
962 Stemmann, L., 2021. Marine snow morphology illuminates the evolution of phytoplankton
963 blooms and determines their subsequent vertical export. Nature communications 12, 2816–
964 2816. https://doi.org/10.1038/s41467-021-22994-4

965 Tutasi, P., Escribano, R., 2020. Zooplankton diel vertical migration and downward C flux into
966 the oxygen minimum zone in the highly productive upwelling region off northern Chile.
967 Biogeosciences 17, 455–473.

968 Uitz, J., Claustre, H., Morel, A., Hooker, S.B., 2006. Vertical distribution of phytoplankton
969 communities in open ocean: An assessment based on surface chlorophyll. Journal of
970 Geophysical Research. C. Oceans 111, [doi:10.1029/2005JC003207].

971 Van Mooy, B.A., Keil, R.G., Devol, A.H., 2002. Impact of suboxia on sinking particulate
972 organic carbon: Enhanced carbon flux and preferential degradation of amino acids via

denitrification. Geochimica et Cosmochimica Acta 66, 457–465.

Vaquer-Sunyer, R., Duarte, C.M., 2008. Thresholds of hypoxia for marine biodiversity. Proceedings of the National Academy of Sciences 105, 15452–15457.

Werner, T., Buchholz, F., 2013. Diel vertical migration behaviour in Euphausiids of the northern Benguela current: seasonal adaptations to food availability and strong gradients of temperature and oxygen. Journal of Plankton Research 35, 792–812.

Wheeler Jr, E., 1967. Copepod detritus in the deep sea. Limnology and Oceanography 12, 697–702.

Wishner, K.F., Ashjian, C.J., Gelfman, C., Gowing, M.M., Kann, L., Levin, L.A., Mullineaux, L.S., Saltzman, J., 1995. Pelagic and Benthic Ecology of the Lower Interface of the Eastern Tropical Pacific Oxygen Minimum Zone. Deep Sea Res. 42, 93–115.

Wishner, K.F., Gelfman, C., Gowing, M.M., Outram, D.M., Rapien, M., Williams, R.L., 2008. Vertical zonation and distributions of calanoid copepods through the lower oxycline of the Arabian Sea oxygen minimum zone. Prog. Oceanogr. 78, 163–191. https://doi.org/10.1016/j.pocean.2008.03.001

Wishner, K.F., Seibel, B., Outram, D., 2020. Ocean deoxygenation and copepods: coping with oxygen minimum zone variability. Biogeosciences 17, 2315–2339.

Wishner, K.F., Seibel, B.A., Roman, C., Deutsch, C., Outram, D., Shaw, C.T., Birk, M.A., Mislan, K., Adams, T., Moore, D., 2018. Ocean deoxygenation and zooplankton: very small oxygen differences matter. Science advances 4, eaau5180.

Yamaguchi, A., Watanabe, Y., Ishida, H., Harimoto, T., Furusawa, K., Suzuki, S., Ishizaka, J., Ikeda, T., Mac Takahashi, M., 2004. Latitudinal differences in the planktonic biomass and community structure down to the greater depths in the western North Pacific. Journal of Oceanography 60, 773–787.

Yamaguchi, A., Watanabe, Y., Ishida, H., Harimoto, T., Furusawa, K., Suzuki, S., Ishizaka, J., Ikeda, T., Takahashi, M., 2002. Community and trophic structures ofpelagic copepods down to greater depths in the western subarctic Paci fic (WEST-COSMIC). Deep Sea Research Part I 49, 1007–1025.

Yasuhara, M., Hunt, G., Dowsett, H.J., Robinson, M.M., Stoll, D.K., 2012. Latitudinal species diversity gradient of marine zooplankton for the last three million years. Ecology Letters 15, 1174–1179. https://doi.org/10.1111/j.1461-0248.2012.01828.x

Table 1: List of the 19 taxa kept for the RDA analysis.

Taxonomic groups	Sub groups
Protista	Protista includes unrecognized protista on the images
Annelida	Images of all Annelida
Chaetognatha	Images of all Chaetognatha
Tunicata	Images of all Gelatinous filter feeders
Cnidaria	Images of all gelatinous carnivores belonging to Cnidaria
Mollusca	Images of all Pteropoda
Cladocera	Images of all Small Cladocera
Eumalacostraca	Images of all Decapoda but those distinguish at detailed taxonomic level
Euphausiacea	Images of all Euphausiacea
Amphipoda	Images of all Amphipoda
Ostracoda	Images of all Ostracoda
Crustacean_larvae	Images of all crustacean larvae
Other_Copepoda	Images of all Copepoda but those distinguish at detailed taxonomic level
Calanoida	Images of all Calanoida but those distinguish at detailed taxonomic level
Oithonidae	Images of all Oithonidae
Corycaeidae	Images of all Corycaeidae
Oncaeidae	Images of all Oncaeidae
Metridinidae	Images of all Metridinidae
Calanidae	Images of all Calanidae

Table 2: Coefficient factors used for equation 1 taken from observed allometric relationships between body area and individual dry mass (Lehette et al., 2009). The conversion factors to carbon are taken from Kiorboe (2013).

Zooplankton category	**Biomass Exponent (*b*)**	**Biomass Multiplier (*a*)**	**DW to C**
Copepods	1.59 ± 0.03	45.25	0.48
Chaetognaths	1.19 ± 0.13	23.45	0.367
Decapods	1.48 ± 0.05	49.58	0.419
Cnidaria	1.02 ± 0.38	43.17	0.132
Tunicata	1.24 ± 0.08	4.03	0.103
Pteropods	1.54 ± 0.03	43.38	0.289
Protists*		0.08 mgC mm^{-3}	
Other (Annelids, Cladocera, Ostracoda)	1.54 ± 0.03	43.38	0.289

* for the protist we used a conversion factor between biovolume and biomass (Biard et al., 2016)

Table 3: Summary of the main mesozooplankton groups global proportion of abundance and biomass:

Taxa Proportion(%)	**Epipelagic**		**Upper Mesopelagic**		**Lower Mesopelagic**	
	Abundance	**Biomass**	**Abundance**	**Biomass**	**Abundance**	**Biomass**
All copepoda	84.89	65	84.80	76.39	94.5	96.5
Chaetognatha	3.67	8.39	2.44	3.48	2.06	2.53
Crust decapoda	2.9	18.9	0.36	14.98	0.00	0.00
Cnidaria	0.7	0.96	0.19	0.24	0.00	0.00
Tunicata	0.5	0.02	0.08	0.001	0.1	0.00
Protista	1.5	0.5	0.97	0.19	0.9	0.09
Pteropoda	1.2	0.6	0.41	0.03	0.00	0.00
Other (annelids, cladocera, ostracoda)	4.2	3.09	10.05	3.23	2.38	0.87

Table 4: Summary of the vertical attenuation rate (b: median and IC: confidence Interval) of mesozooplankton abundance and biomass and particle vertical flux (b: median value and IC: confidence Interval).

	Zooplankton abundance (ind. m^{-3})		**Zooplankton biomass** ($mgC\ m^{-3}$)		**Particle vertical flux** ($mgDW\ m^{-2}\ d^{-1}$)	
	b	IC (95%)	*b*	IC (95%)	*b*	IC (95%)
ANOXIA_TROPIC	-1.82	-2.13 - -1.13	-1.3	-2.9 - -0.75	-0.26	-0.77- -0.19
TROPIC	-1.39	-2.46 - -0.69	-1.04	-1.92 - -0.58	-0.42	-0.78- -0.21
TEMPERATE	-1.19	-1.56 - -0.64	-0.89	-1.26 - -0.57	-0.50	-0.84- -0.11
POLAR	-1.18	-1.71 - -0.96	-0.83	-1.41 - -0.74	-0.78	-4.51- -0.36

Table 5: Probability of H0, no difference between the groups (pairwise Kruskal-Wallis test) for total zooplankton and biomass depth attenuation rates and particle flux attenuation rate. * Significant differences ($p<0.05$).

Two by two comparisons		**Abundance**	**Biomass**	**Flux**
Tropic-Anoxia	Tropic	0.057	0.641	0.77
Tropic-Anoxia	Temperate	0.0018*	0.189	0.82
Tropic-Anoxia	Polar	0.01*	0.238	0.09
Tropic	Temperate	0.34	0.639	0.99
Tropic	Polar	0.51	0.685	0.28
Temperate	Polar	0.99	1	0.52